IEEE Access
Multidisciplinary | Rapid Review | Open Access Journal

Received March 25, 2022, accepted April 28, 2022, date of publication May 2, 2022, date of current version May 9, 2022.

Digital Object Identifier 10.1109/ACCESS.2022.3171811

Chest X-Ray Image Analysis With Combining 2D and 1D Convolutional Neural Network Based Classifier for Rapid Cardiomegaly Screening

JIAN-XING WU[1], CHING-CHOU PAI[2], CHUNG-DANN KAN[3], PI-YUN CHEN[1], WEI-LING CHEN[4], AND CHIA-HUNG LIN[1]

[1]Department of Electrical Engineering, National Chin-Yi University of Technology, Taichung City 41170, Taiwan
[2]Show-Chwan Memorial Hospital, Division of Cardiovascular Surgery, Changhua 500, Taiwan
[3]Division of Cardiovascular Surgery, Department of Surgery, National Cheng Kung University Hospital, College of Medicine, National Cheng Kung University, Tainan City 70101, Taiwan
[4]Ministry of Health Welfare and School of Biomedical Engineering, College of Biomedical Engineering, Institute Food and Drug Administration, Taipei Medical University, Taipei 11031, Taiwan

Corresponding authors: Chung-Dann Kan (kcd5086@gmail.com) and Chia-Hung Lin (eechl53@gmail.com)

This work was supported by the Ministry of Science and Technology, Taiwan, from August 2021 to July 2022, under Contract Most 110-2221-E-006-043 and MOST 110-2221-E-167-005.

ABSTRACT Cardiomegaly is an asymptomatic disease. Symptoms, such as palpitations, chest tightness, and shortness of breath, may be the early indications of cardiac hypertrophy, which can be divided into cardiac hypertrophy and ventricular enlargement. Their causes and treatment strategies are different. The early detection of cardiomegaly can help to make decisions for administering drugs and surgical treatments. In addition, with regard to problems in manual inspection, such as time consuming and the need for human interpretations and experiences, an assistive tool is required to automatically develop and identify normal heart or enlarged hearts. Therefore, this study proposes the combination of 2D (two dimensional) and 1D (one dimensional) convolutional neural network based classifier for rapid cardiomegaly screening in clinical applications based on chest X-ray (CXR) examinations in frontal posteroanterior view. The 2D and 1D convolutional processes and multilayer connected classification network are used to enhance the original CXR image and to remove unwanted noises to increase accuracy in feature extraction and pattern recognition tasks. The training dataset and testing dataset are collected from the National Institutes of Health CXR image database, which is used to train the classifier and validate the performance of the classifier in a K-fold cross-validation manner. Experimental results indicate the potential performance for rapid cardiomegaly screening with regard to recall (%), precision (%), accuracy (%), and F1 score.

INDEX TERMS Cardiomegaly, 2D and 1D convolutional neural network, chest X-ray, cross-validation.

I. INTRODUCTION

An enlarged heart, which is known as cardiomegaly, is not a serious disease, and it may have no signs or symptoms in some people and may have symptoms, such as shortness of breath, abnormal heartbeat (arrhythmia), and edema, in others. Cardiomegaly will cause your heart to pump harder than usual or gradually damage your heart muscle. Congenital heart diseases or abnormal heartbeats can cause heart enlargement, resulting in high blood pressure, heart valve disease, and cardiomyopathy. The risks of complications for cardiomegaly include heart failure, blood clots, heart murmur, and cardiac arrest. Therefore, the first-line chest X-ray (CXR) image [1], [2] is an easy inspection method to directly detect the presence or absence of an abnormality for cardiopulmonary disease detection. This imaging inspection is cost effective, and it has low radiation dose for availability to rapidly screen cardiomegaly. In first-line examination, as seen in Figure 1, the cardiac silhouette can be used to estimate the index of the cardiothoracic ratio (CTR) by

The associate editor coordinating the review of this manuscript and approving it for publication was Taous Meriem Laleg-Kirati.

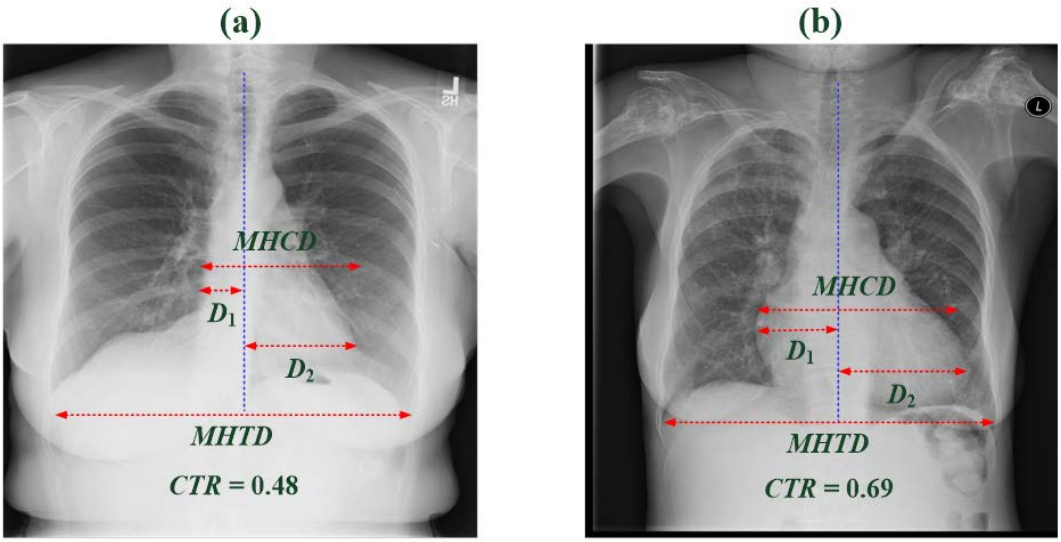

FIGURE 1. Cardiothoracic ratio (CTR) estimation on posteroanterior chest X-ray view (417 × 417 pixels) for normal condition and cardiomegaly. (a) Normal condition (no finding): $CTR = 0.48$, (b) Cardiomegaly: $CTR = 0.69$.

radiologists, which has a 0.50 threshold value for separating the normal condition (no finding) from cardiomegaly [3]–[9]. However, the CTR index is required to select the maximal horizontal cardiac diameter (MHCD) and the maximal horizontal thoracic diameter (MHTD) manually or by using segmentation-based methods (as shown in Figure 1). A CTR index greater than 0.50 indicates the symptoms of enlarged heart. However, manual screening has insufficient human resources, and it is time consuming in medical diagnosis. Given the gray-scale gradient changes in the edges between the lung and heart, segmentation-based methods, such as active shape models, pixel classification, active appearance models, and Harris operator, are used to extrapolate the boundaries of the right/left lung and heart regions in a CXR image. Hence, the heart contour can be critically identified for the desired object location. Then, the feature map of a cardiopulmonary disease can be easily searched with the specific bounding box. However, CXR images may contain noise, and the traditional nonlinear mapping, intensity-based, and gradient-based method is sensitive to noise. It also needs manual manner to determine the MHCD and MHTD for estimating CTR. In addition, digital noise, such as Gaussian noise, Poisson noise, or speckle noise [10]–[12], usually affects the quality of medical images in details and edges, thereby reducing the efficiency of image segmentation, image classification, and pattern recognition tasks. Hence, an image denoising method is necessary to improve the quality of digital medical images.

The noise [10], [11] on CXR images usually contains a low dose of ionizing radiation, which affects the quality of images for cardiopulmonary-related disease diagnoses. Digital filters, wavelet analysis, principal component analysis, and machine learning methods [10] have been proposed to remove such noise and thus improve CXR image quality. However, these methods cannot remove Gaussian and Poisson noise. Hence, to address the abovementioned problems, this study aims to design a multilayer classifier capable of noise filtering, image enhancement, feature extraction, and classification tasks in image preprocessing. Deep-learning-based methods, such as DenseNet (Dense Convolutional Network) [13], ResNet (Residual Network)/FC-ResNets (Fully Convolutional Residual Network) [14], [15], and UNet (Fully Convolutional Network) [16], [17], can be used for feature enhancement, feature extraction, and classification to automatically screen the presence of cardiomegaly on posteroanterior (PA) CXR images.

These multi convolutional-pooling layers and fully connected network can train the end-to-end and pixel-to-pixel image segmentation, which show promising results in this study. These multilayers and classification network can also be used for automated segmentation of liver or tumors based on computed tomography images [6], [18]. They have high performance for multilabel classification applications using the NIH (National Institutes of Health, NIH, Clinical Center) CXR dataset [2], [13]. These 2D fully convolutional neural networks (CNNs) are usually greater than 10 convolutional-pooling layers. Thus, they can perform the image preprocessing and postprocessing tasks to filter noise, enhance the feature map, and then increase the identification accuracy. Through a series of convolution and pooling processes, a multilayer CNN with high capacity for visual object detection can enhance and extract the desired features at different scales and different levels from low-level features (objects' edges or curves) to high-level information (objects' shapes) for detecting nonlinear features. Hence, by increasing the image preprocessing scheme, the network can increase nonlinearity and obtain feature representation. Then, a pooling process with max pooling is used to reduce the sizes of feature maps

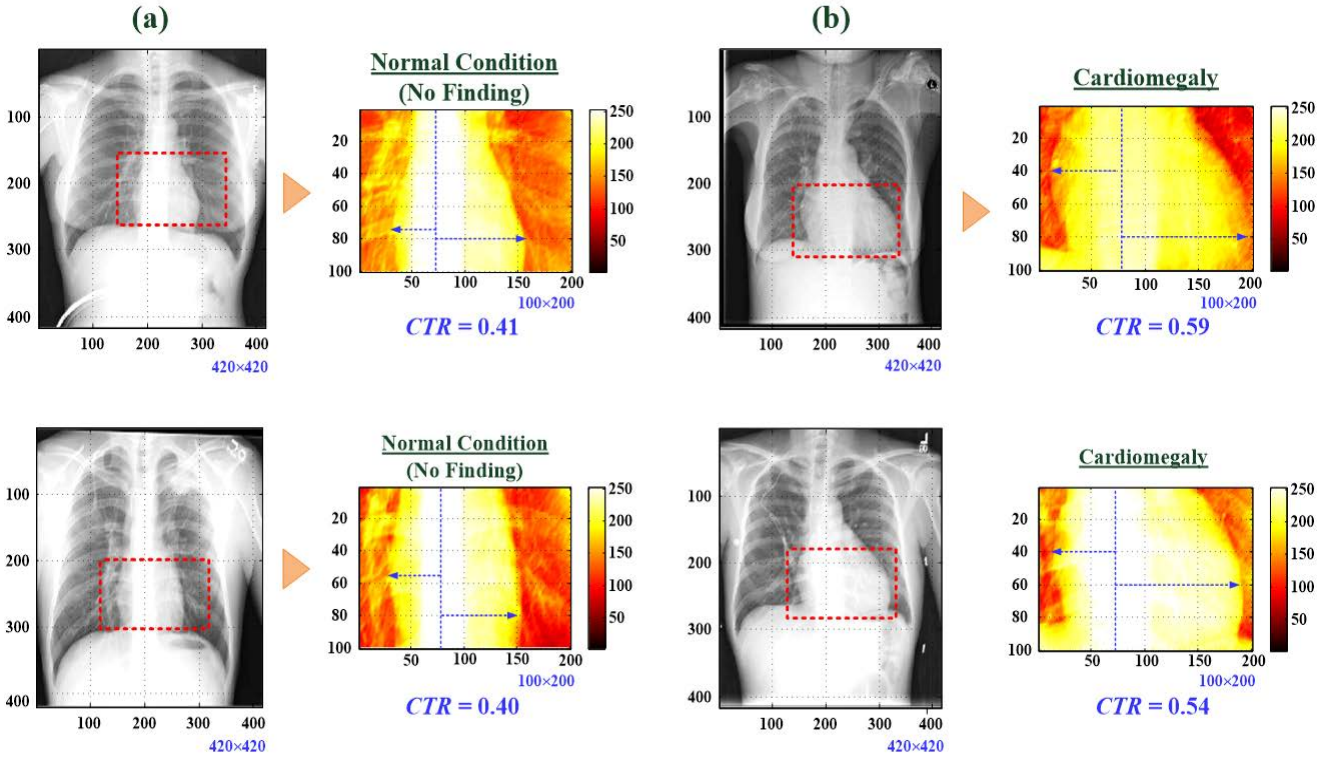

FIGURE 2. Image enhancement and feature map extraction. (a) Feature map for normal condition (no finding, CTR = 0.48), and (b) feature map for cardiomegaly (CTR = 0.69).

for obtaining abstract features and overcome the overfitting matter in the learning stage [19], [20]. Those feature maps can be combined to classify the input CXR images into the possible class. The deep learning (DP)-based CNNs have gradually reduced error rates for classification applications and can also work with noisy data to improve image resolution [21]. However, these processes will increase the complexity levels and have some limitations, such as the determination of a number of convolutional-pooling layers (multilayers), the sizes of convolutional masks ($3 \times 3, 5 \times 5, 7 \times 7, 9 \times 9, 11 \times 11, \ldots$) assignments, large-scale training dataset requirements, high computational complexity for training classifier. In addition, DP-based methods are required on a graphics processing unit (GPU) to accelerate the training tasks with a large amount of training dataset.

Therefore, to simplify the image processing and classification tasks, this study establishes a suitable convolutional-pooling layer and a fully connected network to achieve good accuracy for image classification in cardiomegaly detection. We will utilize the combination of a 2D and one-dimensional (1D) multilayer CNN [14]–[17], [19], [20], [22], consisting of a 2D convolutional layer, flattening layer, 1D convolutional layer, pooling layer, and multilayer classifier in the classification layer. In the first 2D convolutional layer, we use 2D fractional-order-based convolutional processes with different scale fractional-order parameters ($v \in [0, 1]$) [23]–[25] to detect the heart's edge and contour in the specific region. Along the horizontal and vertical directions, two fractional-order-based convolutional windows (with a sliding stride $= 1$) are used to perform spatial convolutional processes for enhancing the heart's feature and removing noises from the original CXR image. With the suitable fractional-order parameters ($v = 0.2 \sim 0.4$) [23]–[25], the heart feature map can be discriminated as the region of interest (ROI) by the spatial convolutional processes for feature extraction. Then, in a ROI, with a specific bounding box, the heart feature map can be easily selected from CXR images. In the flattening layer, the 2D image is converted from matrix presentation to vector presentation as a 1D feature signal by flattening. In the second 1D convolutional layer, a 1D kernel convolutional window (with a sliding stride $= 1$) is subsequently used to deal with the 1D feature signals and can preliminarily quantify the difference levels in feature signals [26]; hence, these feature signals can be distinguished to separate normal conditions from cardiomegaly.

In the classification layer, a fully connected network, consisting of an input layer, pattern layer, summation layer, and output layer [23]–[25], is established as a multilayer classifier to identify cardiomegaly by mapping the relationship between input feature patterns and normal condition (CTR $<$ 0.50) or cardiomegaly (CTR$\geq$ 0.50). The optimization algorithms, such as forward and back propagation (FBP) algorithm [27], [28] and gradient descent algorithm, can be performed in parallel to adjust the network

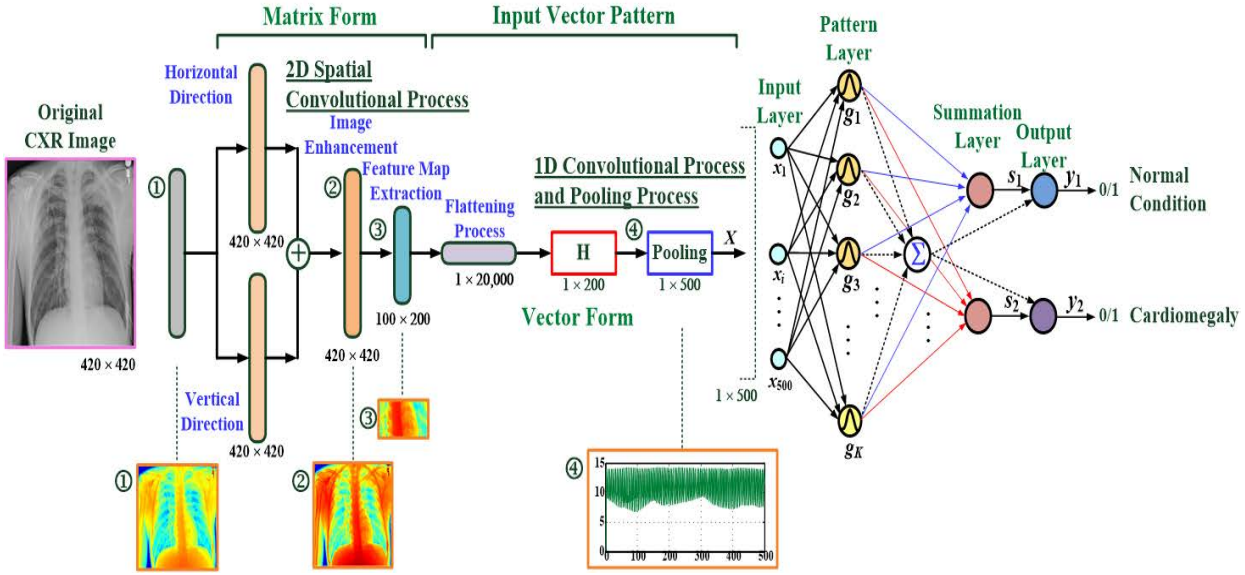

FIGURE 3. Architecture of the proposed novel CNN-based classifier combining 2D and 1D convolutional-neural-network-based classifier for cardiomegaly screening.

parameters in the preceding layer from an output layer to hidden layers. The FBP algorithm has been applied in feed-forward multilayer perceptrons. However, FBP algorithm will incrementally optimize network's overall parameters, including network-connected weights and neuron's biases. The change magnitude with error backpropagation in network parameter adjustment is iteratively updated, resulting in a slow convergence speed and great volatility, making it easy to fall into a local optimum in the training stage [30]. In this study, the gradient descent algorithm [23]–[25] uses the gradient values to refine the optimal network parameter with iteration processes to increase the classification accuracy. We can select an appropriate learning rate to speed up classifier's training processes, and then the convergence speed is also increased. In experimental validations, CXR images are enrolled from the NIH Clinical Center's CXR database [2], [13]. As shown in Figure 1, the labeled "*No Finding*" and "*Cardiomegaly*" images are divided into training and testing datasets to train the proposed classifier in the training stage and validate classifier's feasibility in the recalling stage. Using cross-validation, the experimental results indicated the classification efficiency for automatic cardiomegaly screening on 2D PA CXR images.

The remainder of this study is organized as follows:

Section II describes the methodology, including the experimental setup, CXR image preprocessing, and combining 2D and 1D CNN-based (Novel CNN-based) classifier. Sections III and IV present the feasibility tests and experiment results for clinical applications, and the conclusions, respectively.

II. METHODOLOGY

A. EXPERIMENTAL SETUP

The NIH CXR dataset comprised 112,120 PA X-ray images with disease labels from 30,805 patients (which are collected from 1992 to 2015) [2], [13], which are collected from text radiological reports using natural language processing and are stored in hospitals' picture archiving and communication systems. This medical image database shows common thoracic diseases, which can be detected and located with multilabels by validating using artificial intelligence methods. These disease labels are expected to be $> 90\%$ accurate for supervised learning classification in thorax disease screening. This dataset contains 14 disease labels, such as pneumonia, effusion, infiltration, nodule mass, and cardiomegaly, and one of these labels is cardiomegaly. We will select 200 images from this medical image database, including 100 images with cardiomegaly (positive label) and 100 images with normal condition (no-finding labels). The enlargement of the cardiac silhouette may be due to cardiomegaly, pericardial effusion, or anterior mediastinal mass. The cardiothoracic ratio (CTR) is an aided index to assess the enlargement of the cardiac silhouette, and CTR can be represented as follows [3]–[9]:

$$\mathrm{CTR} = \frac{\mathrm{MHCD}}{\mathrm{MHTD}} \tag{1}$$

$$\mathrm{MHCD} = \mathrm{D}_1 + D_2 \tag{2}$$

where *CTR* is measured on PA CXR view (as seen in Figure 1), which is the ratio of MHCD to MHTD, inner edge of ribs / edge of pleura). A mean index for normal condition is 0.42 – 0.50; < 0.42 indicates pathologic, and $>$ 0.50 is usually used to identify the abnormal conditions for indicating > 0.55 as cardiomegaly and 0.50 to 0.55 as mild cardiomegaly [7], [30], [31]. Hence, CTR can be used as a threshold value for cardiomegaly evaluation. Then, the labeled CXR images can be used to train the deep-learning based CNN as a classifier for separating normal condition from cardiomegaly.

B. CHEST X-RAY IMAGE PREPROCESSING

The CXR images can be converted from Digital Imaging and Communication in a medicine format to a tagged image

file (TIF) format. The TIF is a lossless image format, which can lower the computation time for automatic CXR image examinations. Each size of the CXR image is specified as 1,024 (width) × 1,024 (length) pixels, 8 bites / pixel, with 0 – 255 gray-scale values. In addition, image processing must speed up the pattern recognition task; thus, we need to reduce the sizes of X-ray images before feeding images into the multilayer CNN-based classifier. Hence, we perform rescaling to downscale images from 1,024 × 1,024 pixels to 420 × 420 pixels and maintain sufficient image visual details for indicating heart contours, as shown in the normal condition (no finding) and cardiomegaly in Figure 2. Then, the 100 × 200 bounding box (BB) is used to extract the region of interest (ROI) for obtaining the pathologic information of cardiomegaly, as shown in the gray-scale feature maps in Figure 2.

C. COMBINING 2D AND 1D CONVOLUTIONAL PROCESSES FOR IMAGE ENHANCEMENT AND FEATURE EXTRACTION

In dealing with the 2D CXR image and increasing the classification accuracy, we aim to use 2D and 1D convolutional-pooling processes for image enhancement and feature extraction. In 2D spatial convolutional processes (as seen in Figure 3), two fractional-order convolution (FOC) masks are used to process 2D CXR images and extract low-level features, such as heart's edges and corners. Each fractional-order mask is moved with a stride of 1 (stride = 1) and with zero padding in the horizontal and vertical directions, which can be set as a 3 × 3 sliding window with different fractional-order parameters, $v \in [0, 1]$, to perform the operations of convolutional weights and the general form of the FOC, which can be presented as follows [23]–[25]:

$$FOCI_{xy} = FOC(I_{xy}, M, v)^T \tag{3}$$

where $FOC(\bullet)$ is the fractional-order operator; I_{xy}, $I_{xy} \in [0, 255]$ is the pixel value at location (x, y) in a 2D CXR image, where the image dimension is calculated as $n \times n$, $x = 1, 2, 3, \ldots, n$, and $y = 1, 2, 3, \ldots, n$; $FOCI_{xy}$ is the mapping value at location (x, y); v is the fractional-order parameter. Moreover, based on the Grümwald–Letnikov theory [25], [31], [32], M is the 3 × 3 fractional-order mask, and the mask matrix can be represented as follows:

$$M_x = \begin{bmatrix} 0 & \frac{v^2 - v}{2} & 0 \\ 0 & -v & 0 \\ 0 & 1 & 0 \end{bmatrix}, M_y = M_x^T = \begin{bmatrix} 0 & 0 & 0 \\ \frac{v^2 - v}{2} & -v & 1 \\ 0 & 0 & 0 \end{bmatrix} \tag{4}$$

where M_x and M_y are the FOC masks in the horizontal and vertical directions, respectively. Each FOC mask multiples each element by the corresponding input pixel values, I_{xy}, and then obtains an enhanced feature pattern containing spatial features. The 2D convolution can be performed by a FOC mask in the x direction and then convolving with another FOC mask in the y direction, which act as two low-pass frequency filters [10] and then remove the high-spatial-frequency components from a CXR image. It serves as a smoothing filter for edge detection [23]–[25], [32]. The results of the convolution processes are combined and normalized as follows:

$$FOCI \cong \frac{|FOCI_{xy,x}| + |FOCI_{xy,y}|}{255} \tag{5}$$

where $FOCI_{xy,x}$ and $FOCI_{xy,y}$ are the convolution results in the horizontal and vertical directions, respectively.

After the first image enhancement, using the 100 × 200 BB at the specific region, the feature map of a heart can be extracted from the enhanced CXR image and then can be flattened (FLAT) from a matrix presentation, $FOCI$ (image: 100 × 200), to a vector presentation, $FLATI_x$ (signal: 1 × 20,000). Then, 1D convolutional operator is used to perform the second image enhancement process, and $X[i] = FLATI_x[i]\ ^*H[j]$ (symbol "*" is the convolution operator) can be presented in a discrete–time convolutional form [26]:

$$X[i] = \sum_{j=0}^{M-1} H[j] FLATI_x[i - j] \tag{6}$$

$$H[j] = \exp[\frac{-1}{2}(\frac{j-1}{\sigma})^2] \tag{7}$$

where $X[i]$ is a 1D convolution summation with sampling point, $i = 0, 1, 2, \ldots, N-1$ (the number of sampling point, $N = 20{,}000$ in this study), which is an $N + M - 1$ point signal running from 0 to $N + M - 2$; $H[j]$ is a discrete Gaussian function as a 1D convolution mask with the sliding stride = 1, which is used to enhance the feature of $FLATI_x$ with sampling point, $j = 0, 1, 2, \ldots, M-1$ ($M = 200$ in this study, M is the data length of the 1D convolution mask). After 1D convolution processes, the enhanced signal, X, can be obtained by the summation of all the multiplications of the first enhanced signal, $FLATI_x[i - j]$, and the weighted values of $H[j]$; then, pooling is used to reduce feature signal dimension, which can be expressed as follows:

$$x[i] = X[40i], i = 1, 2, 3, \ldots, n' \tag{8}$$

$$n' \approx \frac{N + M - 2}{40} \tag{9}$$

where $x[i]$ is the subsampling feature signal obtained with a sliding stride = 40. Hence, the vector dimension of the feature signal can be reduced from $N + M - 2$ to n' without zero-padding ($n' \approx 500$). As seen in Figure 4, for feature maps of normal condition (CTR $\leq$ 0.50) and cardiomegaly (CTR$>$ 0.50), the number of feature parameters is reduced to $\approx$ 25% of the total number of a feature map, and can retain key feature, which can reduce the computational complexity. In addition, as shown in Figure 4, feature maps in vector form (as 1D feature signals) are used to preliminarily quantify the different levels (red and green feature maps) for further classification applications.

D. MULTILAYER CLASSIFIER IN CLASSIFICATION LAYER

In the classification layer (as seen in Figure 3), a multilayer connected network, consisting of an input layer, a pattern layer, a summation layer, and an output layer, is used to

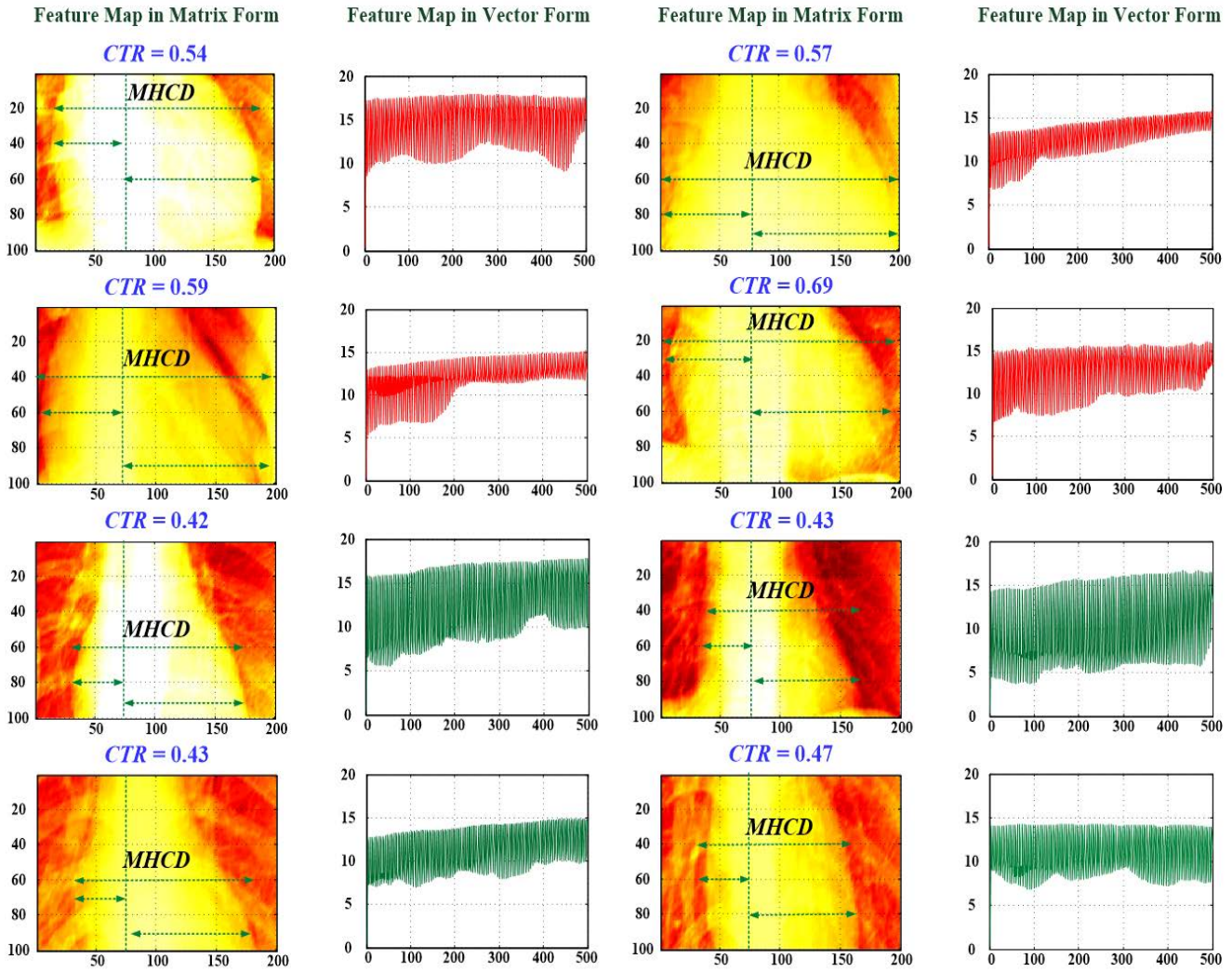

FIGURE 4. Feature maps for normal condition (CTR ≤ 0.50) and cardiomegaly (CTR > 0.50) as representations in matrix forms and vector forms.

establish a classifier with a feeding feature signal for further cardiomegaly screening. The pattern layer can map the 1D feature signal and output into a high-dimension space by using a linear combiner. Hence, the output of the pattern layer can be represented as follows:

$$y_k(x) = \sum_{k=1}^{K} w_{ki} g_k(x_i), i = 1, 2, 3, \ldots, n' \tag{10}$$

$$g_k(x_i) = \exp[-\sum_{k=1}^{K} \frac{(x_i - w_{ki})^2}{2\sigma_k^2}] \tag{11}$$

where w_{ki} is the network-weighted values between the input layer and pattern layer, as a matrix $W = [w_{ki}]K \times n\prime(n\prime = 500)$, which can be set by using $K \times 500$ input training feature signals. Classifier's output can be normalized as follows:

$$y_j = \frac{\sum_{k=1}^{K} w_{kj} y_k(x)}{\sum_{k=1}^{K} g_k(r_k)} = \sum_{k=1}^{K} w_{kj} u, u = \frac{y_k(x)}{\sum_{k=1}^{K} g_k(r_k)} \tag{12}$$

where $Y(k) = [y_1(k), y_2(k), 1]$ is the network-weighted values between the pattern layer and summation layer, which can be set by $K \times 3$ output training patterns, encoded as (1) *Normal Condition*: [1, 0, 1] and (2) *Cardiomegaly*: [0, 1, 1].

In training the classifier, identifying the smoothing parameter is required, σ_k, $\sigma = \sigma_1 = \ldots = \sigma_k = \ldots = \sigma_K$, to minimize the function of mean squared error (MSE) for multiclass classification:

$$MSE = \frac{1}{K} \sum_{k=1}^{K} (t_j - y_j)^2 \leq \varepsilon \tag{13}$$

where t_j is the jth desired target outputs referring to the input signals in the training dataset; $T = [t_1, t_2]$ for multiple classes, and $\varepsilon \in (0, 1)$ is a tolerance error. The gradient descent method is used to adjust the optimal parameter, σ_{opt}, using the iteration computations [25], [26], [32], and the gradient values can be computed as follows:

$$\nabla = \frac{\partial \text{MSE}}{\partial \sigma} \approx (t_j - y_j)(\frac{\frac{\partial s_j}{\partial \sigma} - y_j \frac{\partial g_k}{\partial \sigma}}{g_k}) \tag{14}$$

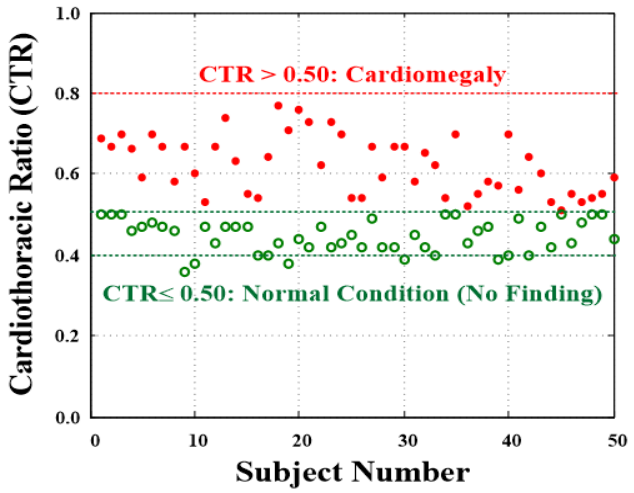

FIGURE 5. Distributions and statistics of normal condition and cardiomegaly for 100 enrolled subjects.

$$\begin{cases} \dfrac{\partial s_j}{\partial \sigma} = 2\left(\sum_{k=1}^{K} w_{ki} g_k\right)\left(\dfrac{(x_i - w_{ki})^2}{2\sigma^3}\right) & (15) \\ \dfrac{\partial g_k}{\partial \sigma} = 2\left(\sum_{k=1}^{K} g_k\right)\left(\dfrac{(x_i - w_{ki})^2}{2\sigma^3}\right) & (16) \end{cases}$$

Hence, the optimal parameter, σ_{opt}, can be refined using the iteration computation:

$$\sigma(p+1) = \sigma(p) - \eta\nabla \quad (17)$$

where η is the learning rate, $0 < \eta \leq 1$; p is the number of iteration computations, $p = 0, 1, 2, 3, \ldots, p_{max}$, and p_{max} is the maximum iteration number. The optimal parameter, σ_{opt}, can be used to minimize the function of *MSE*.

III. EXPERIMENTAL RESULTS AND DISCUSSION

The NIH CXR image dataset [2], [13] was used to validate the intended medical purpose and evaluate the proposed combining 2D and 1D CNN-based classifier for two-class classification. Each enrolled image was resized from 1,024 × 1,024 pixels to 420 × 420 pixels (96 dpi, with a bit depth of 32 bits), which were converted from digital imaging and communication in a medicine format to a tagged image file (TIF) format. The TIF format is a lossless image that could lower the computation time [24]. Figure 5 shows the distributions and statistics of normal condition (CTR≤ 0.50) and cardiomegaly (CTR>0.50) for 100 enrolled subjects. Given a specific BB with 100 × 200 pixels, feature maps could be screenshot from the 100 CXR images and then could be used to train the proposed classifier. In an automatic cardiomegaly screening design (as seen in Figure 6), four processes were identified: (1) CXR image enhancement using 2D spatial fractional-order convolutional processes, (2) feature map extraction (ROI), (3) 1D convolutional pooling, and (4) cardiomegaly screening with the combination of 2D and 1D CNN-based classifier. The proposed digital image process and classifier algorithms were implemented on a tablet PC using a high-level graphical programming language in LabVIEW and MATLAB software (NI^{TM}, Austin, TX, USA), and the GPU (NVIDIA®GeForce®RTX^{TM}2080 Ti, 1755 MHz, 11 GB GDDR6) was used to speed up the executed time for digital image processing and pattern recognition tasks. Table 1 shows the related data of the proposed multilayer classifier, including its layer functions, manners, and feature maps. The feasibility study was validated as described in detail in the subsequent sections.

A. FEASIBILITY TESTS FOR THE PROPOSED MULTILAYER CLASSIFIER

For the 200 enrolled subjects from the NIH CXR image database, we extracted 200 feature maps using the 2D convolutional process and 1D convolutional pooling, including 100 normal map and 100 abnormal maps for cardiomegaly. In this study, we randomly selected 100 trained feature maps to train the multilayer classifier in the learning stage. Then, using 100 pairs of input–output feature maps, we established a fully connected topology network, consisting of 500 input nodes, 100 pattern nodes, three summation nodes, and two output nodes in the classification layer (as seen in Figure 3 and Table 1). In the literature [23]–[25], the 3 × 3 fractional-order convolutional mask using fractional-order parameters $v = 0.20 - 0.40$, ($v = 0.30$ was selected) could yield promising results for image enhancement and remove noise [23]–[25], as shown in Figure 7. Hence, the heart's edge and contour could be identified and then easily selected from a CXR image. Then, in the feature extraction layer, 1D convolutional pooling was used to extract the feature patterns in vector form and reduce the feature parameters, thereby addressing overfitting in the learning stage. The trained feature maps (as shown in Figure 4) were fed into the classifier, and the convergent condition was set as the tolerance value, $\varepsilon \leq 10^{-2}$, and the initial condition, that is, $\sigma_0 = 1.0000$. Furthermore, the gradient descent method was used to adjust the smoothing parameter in the pattern layer to minimize the *MSE* function using the iteration computations. Figures 8(a) and 8(b) show the training history curves for the proposed classifier, as optimal parameters and *MSE*s versus iteration numbers, respectively. Using different learning rates, $\eta = 0.3 - 0.6$, and the gradient descent method required < 20 iterative computations to reach the specific convergent condition. Given these optimal solutions (Figure 8(b)), the optimal parameter, $\sigma_{opt} \approx 0.0.0581$, could minimize the *MSE* function and increase the classification accuracy in the learning stage (100% accuracy). The overall iteration computations reached an average CPU time of 4.8430 s to refine the optimal parameter. Hence, the proposed classifier showed feasibility for automatic cardiomegaly screening using PA CXR images in clinical applications

B. CROSS-VALIDATION TESTS FOR PROPOSED MULTILAYER CLASSIFIER

For feasibility tests in clinical applications, the collected feature maps were divided into two groups, including the

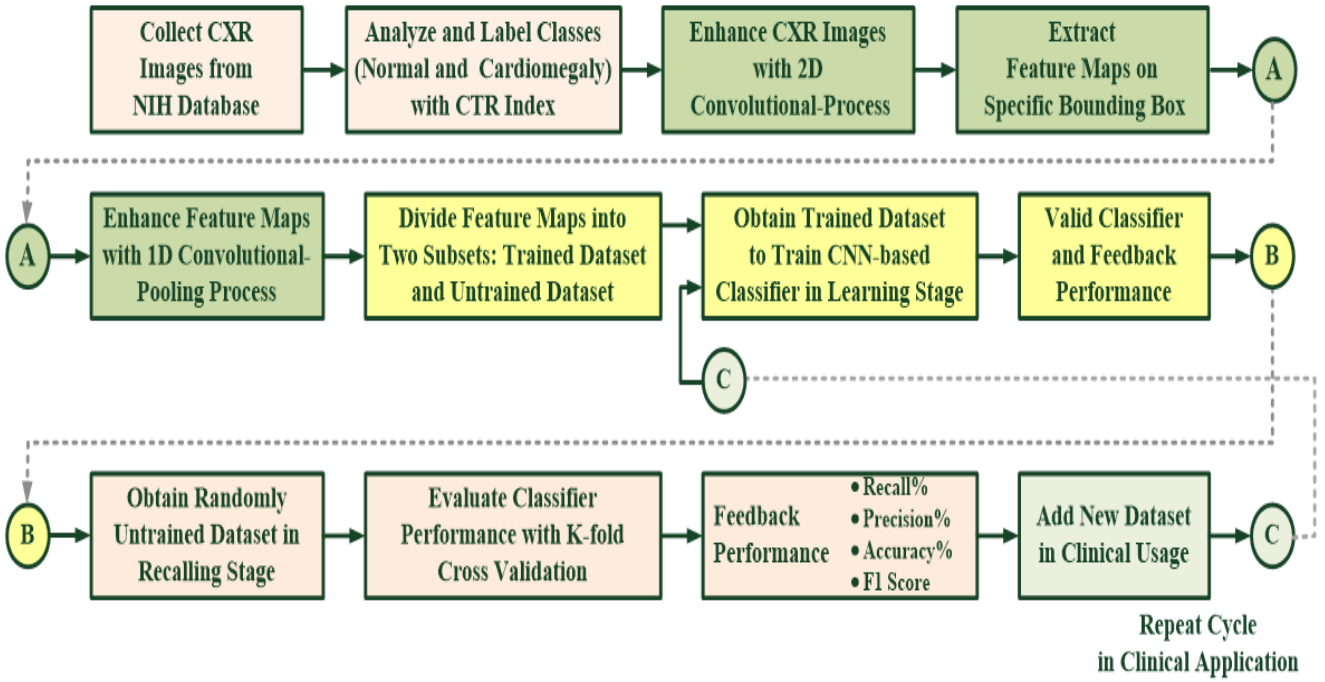

FIGURE 6. Flowchart of automatic cardiomegaly screening design for clinical applications.

TABLE 1. Related data of the proposed combining 2D and 1D CNN-based multilayer classifier.

Layer Function	Manner	Feature Map
Image Enhancement Layer	2D Spatial Fractional-Order Convolutional Processes (3 × 3 Fractional-Order Convolutional Mask, Stride = 1)	$FOCI$ (420 × 420)
1st Feature Extraction Layer	With 100 × 200 Bounding Box and Flattening Process	$FLATI_x$ (1 × 20,000)
2nd Feature Extraction Layer	1D Convolutional Process with Discrete Gaussian Function (Data Length of Convolution Mask, M=200, Stride = 1)	X(1 × 20,200)
Simplifying Feature Layer	1D Pooling Processes (Stride = 40)	x (1 × 500)
Classification Layer	Multi-Layer Classifier: 500 input nodes, 100 pattern nodes, 3 summation nodes, 2 output nodes	Input Pattern of Fully Connecting Network: [x] (1 × 500)
	Learning Algorithm: Gradient Descent Method	

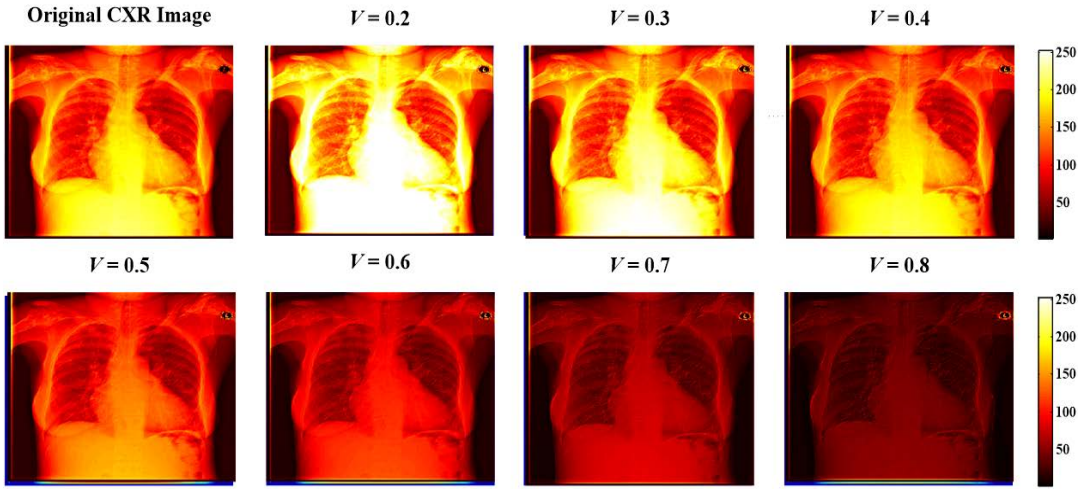

FIGURE 7. Image enhancement via 2D spatial convolution with fractional-order parameters, $v = 0.2 - 0.8$, for CXR image.

trained dataset and untrained dataset, and then the trained and untrained feature maps were randomly selected to train the classifier, which was used to validate the classifier by performing 10-fold cross-validation. As shown in Table 2,

TABLE 2. Evaluation criteria of the proposed classifier, including precision (%), recall (%), accuracy (%), and F1 score.

		Actual		Total	Precision (%)
		Positive	Negative		
Predicted	Positive	TP	FP	TP + FP	(TP) / (TP + FP)
	Negative	FN	TN	FN +TN	
Total		TP + FN	FP + TN	Accuracy (%): (TP + TN) / (TP + FP + TN + FN)	
Recall (%)		(TP) / (TP + FN)			
F1 Score		(2TP) / (2TP + FP + FN)			

Note: (1) TP: true positive, (2) TN: ture negative, (3) FP: false positive.. (4) FN: false negative

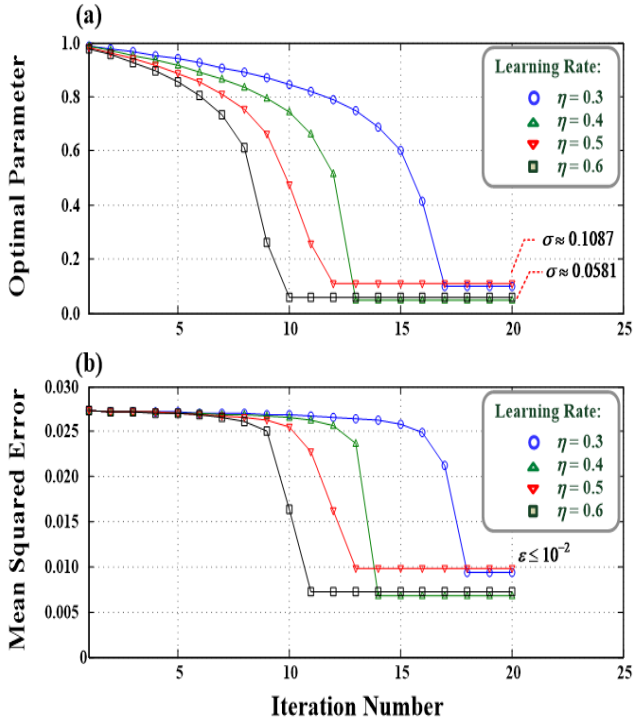

FIGURE 8. Training history curves for the proposed multilayer classifier. (a) Optimal parameters versus iteration numbers with different learning rates, and (b) mean squared error versus iteration numbers with different learning rates.

four criteria were used to evaluate the proposed classifier model, including precision (%), recall (%), accuracy (%), and F1 score indexes [23], [32]. Accuracy (%) was an index to measure the percentage of correct classification; thus, a classifier had been established in the recalling stage. For screening positive cases, we could observe that the recall (%) index, which indicated the number of positive cases, could be predicted. The precision (%) index was also known as the positive predictive value (PPV), which indicated the number of positive cases (including the correct percentage). The F1 score index was a harmonic mean of the precision (%) and recall (%) (combining the precision and recall into a single screening metric), which indicated that the F1 score provided equal weight to precision and recall, including the errors of false positives and false negatives; a classifier could obtain a high F1 score, whereas both precision (%) and recall (%) had high values.

After training the classifier using 100 trained feature maps, 100 untrained feature maps, including 50 for normal subjects and 50 for cardiomegaly subjects, were randomly selected from the dataset to validate the classifier. Using the same validation process, 10-fold cross-validations were performed; the experimental results of the proposed classifier are shown in Table 3, with an average precision (%) of 97.60% and an average recall (%) of 99.20% for predicted abnormality and correctly identified abnormality (true positive [TP] for $CTR > 0.50$), respectively, an average accuracy of 98.40% for correctly identified normal and cardiomegaly, and an average F1 score of 0.9838 for the proposed classifier performance on classification tasks, which was greater than 0.9000, indicating the potential application of the classification model. In addition, recall (%) as an index of PPV, was greater than 80% based on the predictive performance of the classifier. Hence, we could recommend the combination of 2D and 1D CNN-based classifier to automatically screen the presence of cardiomegaly on PA CXR images in clinical applications.

C. DISCUSSION

Experimental tests showed promising results for the proposed classifier in automatic cardiomegaly screening using PA CXR images. In addition, the 10-fold cross-validations were performed, as seen in Table 3, and the manual method with CTR estimation (using equations (1) and (2)) in 100 CXR images had good reproducibility and accuracy, with average CTRs of 0.4377 and 0.6307 for identified normal condition and cardiomegaly, respectively. Using the related classifier's data in Table 4, we also established a multilayer 2D CNN-based classifier consisting of a fractional-order convolutional layer with two convolution masks (Stride = 1), a kernel convolutional layer with 16 kernel convolution masks (Stride = 1), 16 maximum pooling masks (Stride = 2) in a pooling layer, a flattening layer, and a fully connecting classification network (multi-layer perceptron). The fully connecting network consisted of an input layer (1, 250 nodes), two hidden layers (168 and 64 nodes), and an output layer (2 nodes). The 2D CNN-based classifier was implemented using the open source Tensorflow platform (Version 1.9.0) in Python [33], [34]. The same trained and untrained feature maps with 10-fold cross-validation obtained an average precision of 97.80%, an average recall of 98.20% for predicting the possible cardiomegaly and correctly identifying TP, an average accuracy

TABLE 3. Experimental results of 10-fold cross validation for the proposed multilayer classifier.

Fold	Precision (%)	Recall (%)	Accuracy (%)	F1 Score	Average CTR for Normal	Average CTR for Cardiomegaly
1	100.00 (TP: 50, FP: 0)	100.00 (TP: 50, FN: 0)	100.00	1.0000	0.4452 ± 0.0383	0.6556 ± 0.0725
2	100.00 (TP: 50, FP: 0)	100.00 (TP: 50, FN: 0)	100.00	1.0000	0.4476 ± 0.0399	0.5900 ± 0.0579
3	96.00 (TP: 48, FP: 2)	96.00 (TP: 48, FN: 2)	96.00	0.9600	0.4416 ± 0.1212	0.6496 ± 0.0754
4	96.00 (TP: 48, FP: 2)	100.00 (TP: 48, FN: 0)	98.00	0.9796	0.4336 ± 0.0323	0.6452 ± 0.07621
5	100.00 (TP: 50, FP: 0)	100.00 (TP: 50, FN: 0)	100.00	1.0000	0.4380 ± 0.0338	0.6320 ± 0.0786
6	92.00 (TP: 46, FP: 4)	100.00 (TP: 50, FN: 0)	96.00	0.9583	0.4320 ± 0.0336	0.5780 ± 0.0532
7	96.00 (TP: 48, FP: 2)	96.00 (TP: 48, FN: 2)	96.00	0.9600	0.4348 ± 0.0344	0.6296 ± 0.0778
8	96.00 (TP: 48, FP: 2)	100.00 (TP: 48, FN: 0)	98.00	0.9796	0.4384 ± 0.0342	0.6436 ± 0.0758
9	100.00 (TP: 50, FP: 0)	100.00 (TP: 50, FN: 0)	100.00	1.0000	0.4380 ± 0.0338	0.6384 ± 0.0779
10	100.00 (TP: 50, FP: 0)	100.00 (TP: 50, FN: 0)	100.00	1.0000	0.4280 ± 0.0312	0.6448 ± 0.0747
Average	97.60	99.20	98.40	0.9838	0.4377	0.6307

of 98.00% for correctly identifying normal condition and cardiomegaly, and an average F1 score of 0.9799 for verifying the classifier performance. The proposed multilayer classifier also performed better than the multilayer 2D CNN-based classifier, as shown by the experimental results in Table 4. However, the multilayer 2D CNN required more feature parameters for trained the classifier and then increased high computational complexity with the iteration computations. In addition, the GPU needed to accelerate the training process and parallelize computations with the multi convolution and pooling processes. It took an average CPU time of < 300 s for training the classifier. Hence, under the same multilayer architecture, the performance of the proposed multilayer classifier was superior to that of the 2D CNN-based classifier. In specific, the proposed multilayer classifier had less feature parameter requirement in the 2D convolutional layer, simpler linear weighted sums for the 1D convolutional process to deal with the 1D feature signals, and simpler classifier implement process compared with the 2D CNN-based classifier.

In clinical diagnosis, clinicians and radiologists could rapidly use visual inspection to identify the normality or abnormality on PA CXR images and then compute the CTR indexes. However, manual inspection was time consuming, and the diagnostic results were dependent on readers' interpretations and experiences. The proposed combination of 2D and 1D CNN-based classifier's diagnostic tests took less than 2 s CPU time in dealing with 100 CXR images. Hence, automatic screening could address the insufficient human resources for manual screening and allow clinicians and radiologists to focus on follow-up medical strategies. Some advantages of the proposed classifier are shown below:

- The feature maps could be enhanced in 2D spatial convolutional processes by identifying the heart's edge and contour and removing noise;
- The feature maps in vector form (as feature signals) were used to quantify the different levels for separating the normal condition from cardiomegaly.
- The dimension of feature patterns could be reduced to improve the overfitting problems;
- The multilayer classifier could be easily established by the trained dataset with the key input-output paired feature maps and easily implemented using high-level programming languages (Language C/C++ or MATLAB software).

In addition, the proposed classifier had a limitation in identifying heart enlargement or myocardial hypertrophy. The determination of the heart size, such as four chambers (ventricles and atriums), was an important measurement parameter to evaluate potential cardiomegaly. Cardiac echocardiography (CECHO), cardiac magnetic resonance imaging (CMRI), and cardiac computed tomography (CCT) [35]–[38] were superior to chest radiography, which provided good imaging to assess the heart chamber size and determine the heart chamber. The results of CECHO showed promising sensitivity and specificity in determining cardiac chamber sizes [36], [39], as the gold standard, and high correlation between CTR indexes and heart sizes. Compared with the expensive manners, such as CMRI and CCT, this study recommended that the CXR images were easy and cheap; thus, it could directly estimate the CIR index for heart size measurement in preliminary examination during first-line examination; hence, during automatic screening tool verification, the larger the F1 score ($> 95\%$), the proposed multilayer classifier had

TABLE 4. Related data the multilayer 2D CNN-based classifier and experimental results of 10-fold cross validation.

Input CXR Image	420 pixels × 420 pixels
1st convolutional layer	2 convolution masks, 3 × 3 fractional-order convolution mask (420 pixels × 420 pixels), Stride = 1
2nd convolutional layer	16 convolution masks, 3 × 3 kernel convolution mask (100 pixels × 200 pixels) , Stride = 1
2nd pooling layer	16 pooling masks, 2 × 2 maximum pooling mask (25 pixels × 50 pixels) , Stride = 2
Flattening layer	1 × 1,250 feature vector
Classifier's input layer	1 × 1,250 input vector (1,250 input nodes)
1st hidden layer	168 hidden nodes
2nd hidden layer	64 hidden nodes
Classifier's output layer	2 output nodes (for normality and abnormality)
Average Precision (%)	97.80%
Average Recall (%)	98.20%
Average Accuracy (%)	98.00%
Average F1 Score	0.9799

the better performance in separating the normal condition from cardiomegaly and the greater its authenticity for an informed decision.

IV. CONCLUSION

We developed a combining 2D and 1D CNN-based classifier with CXR images to identify the disease present in normal condition or cardiomegaly during first-line examination, and the performance of the proposed classifier was also validated. In the convolutional layer, the sequence of 2D fractional-order and 1D kernel convolutional processes was used to enhance the image and remove unwanted noise, which could help to extract the 2D feature maps with specific BB and to transform into 1D feature signals for further classification tasks. Flattening and 1D pooling processes could reduce the dimension of the feature map, leading to low computational operations for real-time digital image processes and pattern recognition tasks. Using 10-fold cross-validation, randomly untrained feature map was fed into the classifier, and its pattern recognition scheme showed promising results in separating the normal condition from the cardiomegaly, as the average recall, average precision, average accuracy, and average F_1 score were greater than 95% for screening abnormalities. The experimental results indicated that the training model, computational efficiency, and automatic screening were better than the manual method in clinical application. Training and examining the classifier and CXR images would take less than 5.0 s. Using image examinations, such as CECHO, CMRI, and CCT [35]–[38], the four chambers of the heart could be accurately estimated to evaluate the enlarged heart or myocardial hypertrophy (left ventricular hypertrophy). Considering the absence of pain or immediate risk, the above imaging manners were a potential way to measure heart size, muscle thickness, and pumping function to discover cardiomegaly, such as left and right ventricular hypertrophy. Routine chest radiography could also rapidly inspect dilated cardiomyopathy, which might increase heart size on a CXR image, such as right/left atrial shadow (atrial enlargement) or right / left ventricular hypertrophy (ventricular enlargement) [40], [41]. Therefore, the proposed multilayer classifier could replace the manual manner for tasks requiring specific expertise and experience (clinicians and radiologists) for medical image examinations. In addition, the trained dataset could be divided into four classes, including normal condition (CTR $\leq$ 0.50), mild cardiomegaly (0.50 $<$ CTR $\leq$ 0.55), moderate cardiomegaly (0.55 $<$ CTR $\leq$ 0.60) [7], [8], and severe cardiomegaly to train the proposed classifier, which could maintain its intended medical purpose in real-world application and could also raise its indication in clinical applications as a computer-aided decision-making tool.

ACKNOWLEDGMENT

The enrolled image dataset was collected from National Institutes of Health (NIH) Clinical Center Chest X-ray Database.

ABBREVIATIONS

CXR	Chest X-Ray
CTR	Cardio-Thoracic Ratio
MHCD	Maximal Horizontal Cardiac Diameter
MHTD	Maximal Horizontal Thoracic Diameter
DenseNet	Dense Convolutional Network
ResNet	Residual Network
FC-ResNets	Fully Convolutional Residual Network
U-Net	Fully Convolutional Network
PA	Posteroanterior
CT	Computed Tomography
NIH	National Institutes of Health
CNN	Convolutional Neural Network
FBP	Forward and Back Propagation
BB	Bounding Box
ROI	Region of Interest
FOC	Fractional-Order Convolution

FLAT	Flattened
PPV	Positive Predictive Value
CECHO	Cardiac Echocardiography
CMRI	Cardiac Magnetic Resonance Imaging
CCT	Cardiac Computed Tomography

REFERENCES

[1] E. Sogancioglu, K. Murphy, E. Calli, E. T. Scholten, S. Schalekamp, and B. Van Ginneken, "Cardiomegaly detection on chest radiographs: Segmentation versus classification," *IEEE Access*, vol. 8, pp. 94631–94642, 2020.

[2] I. M. Baltruschat, H. Nickisch, M. Grass, T. Knopp, and A. Saalbach, "Comparison of deep learning approaches for multi-label chest X-ray classification," *Sci. Rep.*, vol. 9, no. 1, pp. 1–10, Dec. 2019.

[3] N. Sezaki and K. Ukena, "Automatic computation of the cardiothoracic ratio with application to mass screening," *IEEE Trans. Biomed. Eng.*, vol. BE-20, no. 4, pp. 248–259, Jul. 1974.

[4] K. Dimopoulos, G. Giannakoulas, I. Bendayan, E. Liodakis, R. Petraco, G.-P. Diller, M. F. Piepoli, L. Swan, M. Mullen, N. Best, P. A. Poole-Wilson, D. P. Francis, M. B. Rubens, and M. A. Gatzoulis, "Cardiothoracic ratio from postero-anterior chest radiographs: A simple, reproducible and independent marker of disease severity and outcome in adults with congenital heart disease," *Int. J. Cardiol.*, vol. 166, no. 2, pp. 453–457, Jun. 2013.

[5] M. Cicero, A. Bilbily, E. Colak, T. Dowdell, B. Gray, K. Perampaladas, and J. Barfett, "Training and validating a deep convolutional neural network for computer-aided detection and classification of abnormalities on frontal chest radiographs," *Invest. Radiol.*, vol. 52, no. 5, pp. 281–287, 2017.

[6] Z. Li, Z. Hou, Z. Hao, Y. An, S. Liang, B. Lu, and C. Chen, "Automatic cardiothoracic ratio calculation with deep learning," *IEEE Access*, vol. 7, pp. 37749–37756, 2019.

[7] P. Simkus, M. G. Gimeno, A. Banisauskaite, J. Noreikaite, D. McCreavy, D. Penha, and M. Arzanauskaite, "Limitations of cardiothoracic ratio derived from chest radiographs to predict real heart size: Comparison with magnetic resonance imaging," *Insights Imag.*, vol. 12, no. 1, pp. 1–10, Dec. 2021.

[8] K. Truszkiewicz, R. Poreba, and P. Gac, "Radiological cardiothoracic ratio in evidence-based medicine," *J. Clin. Med.*, vol. 10, pp. 1–9, Jan. 2021.

[9] W. Chaisangmongkon, I. Chamveha, T. Promwiset, P. Saiviroonporn, and T. Tongdee, "External validation of deep learning algorithms for cardiothoracic ratio measurement," *IEEE Access*, vol. 9, pp. 110287–110298, 2021.

[10] D. N. H. Thanh, P. Kalavathi, L. T. Thanh, and V. B. S. Prasath, "Chest X-ray image denoising using Nesterov optimization method with total variation regularization," *Proc. Comput. Sci.*, vol. 171, pp. 1961–1969, Jan. 2020.

[11] D. Thanh, P. Surya, and L. M. Hieu, "A review on CT and X-ray images denoising methods," *Informatica*, vol. 43, no. 2, pp. 151–159, Jun. 2019.

[12] A. Saadia and A. Rashdi, "A speckle noise removal method," *Circuits, Syst., Signal Process.*, vol. 37, no. 6, pp. 2639–2650, Jun. 2018.

[13] X. Wang, Y. Peng, L. Lu, Z. Lu, M. Bagheri, and R. M. Summers, "ChestX-ray8: Hospital-scale chest X-ray database and benchmarks on weakly-supervised classification and localization of common thorax diseases," in *Proc. IEEE Conf. Comput. Vis. Pattern Recognit. (CVPR)*, Honolulu, HI, USA, Jul. 2017, pp. 2097–2106.

[14] K. He, X. Zhang, S. Ren, and J. Sun, "Deep residual learning for image recognition," in *Proc. IEEE Conf. Comput. Vis. Pattern Recognit.*, vol. 1, Jun. 2016, pp. 770–778.

[15] M. Drozdzal, E. Vorontsov, G. Chartrand, S. Kadoury, and C. Pal, *The Importance of Skip Connections in Biomedical Image Segmentation* (Lecture Notes in Computer Science). Cham, Switzerland: Springer, 2016.

[16] E. Shelhamer, J. Long, and T. Darrell, "Fully convolutional networks for semantic segmentation," *IEEE Trans. Pattern Anal. Mach. Intell.*, vol. 39, no. 4, pp. 640–651, Apr. 2017.

[17] Q. Que, Z. Tang, R. Wang, Z. Zeng, J. Wang, M. Chua, T. S. Gee, X. Yang, and B. Veeravalli, "CardioXNet: Automated detection for cardiomegaly based on deep learning," in *Proc. 40th Annu. Int. Conf. IEEE Eng. Med. Biol. Soc. (EMBC)*, Jul. 2018, pp. 612–615.

[18] M. Drozdzal, G. Chartrand, E. Vorontsov, M. Shakeri, L. D. Jorio, A. Tang, A. Romero, Y. Bengio, C. Pal, and S. Kadoury, "Learning normalized inputs for iterative estimation in medical image segmentation," *Med. Image Anal.*, vol. 44, pp. 1–13, Feb. 2018.

[19] J. Gu, Z. Wang, J. Kuen, L. Ma, A. Shahroudy, B. Shuai, T. Liu, X. Wang, G. Wang, J. Cai, and T. Chen, "Recent advances in convolutional neural network," *Pattern Recognit.*, vol. 77, pp. 354–377, May 2018.

[20] S. Kiranyaz, O. Avci, O. Abdeljaber, T. Ince, M. Gabbouj, and J. Daniel Inman, "1D convolutional neural networks and applications: A survey," *Mech. Syst. Signal Process.*, vol. 151, Apr. 2021, Art. no. 107398.

[21] M. E. Lindquist, M. J. Gosnell, K. S. Khan, L. J. Byl, W. Zhou, J. Jiang, and J. J. Vettukattilb, "3D printing in cardiology: A review of applications and roles for advanced cardiac imaging," *Ann. 3D Printed Med.*, vol. 4, Dec. 2021, Art. no. 100034.

[22] D. K. Appana, W. Ahmad, and J.-M. Kim, "Speed invariant bearing fault characterization using convolutional neural networks," in *Proc. Int. Workshop Multi-Disciplinary Trends Artif. Intell. (MIWAI)*, 2017, pp. 189–198.

[23] J.-X. Wu, P.-Y. Chen, C.-M. Li, Y.-C. Kuo, N.-S. Pai, and C.-H. Lin, "Multilayer fractional-order machine vision classifier for rapid typical lung diseases screening on digital chest X-ray images," *IEEE Access*, vol. 8, pp. 105886–105902, 2020.

[24] C.-H. Lin, C.-D. Kan, W.-L. Chen, and P.-T. Huang, "Application of two-dimensional fractional-order convolution and bounding box pixel analysis for rapid screening of pleural effusion," *J. X-Ray Sci. Technol.*, vol. 27, no. 3, pp. 517–535, Jul. 2019.

[25] C.-H. Lin, J.-X. Wu, C.-M. Li, P.-Y. Chen, N.-S. Pai, and Y.-C. Kuo, "Enhancement of chest X-ray images to improve screening accuracy rate using iterated function system and multilayer fractional-order machine learning classifier," *IEEE Photon. J.*, vol. 12, no. 4, pp. 1–9, Jul. 2020.

[26] C.-H. Lin, J.-X. Wu, C.-D. Kan, P.-Y. Chen, and W.-L. Chen, "Arteriovenous shunt stenosis assessment based on empirical mode decomposition and 1D-convolutional neural network: Clinical trial stage," *Biomed. Signal Process. Control*, vol. 66, Apr. 2021, Art. no. 102461.

[27] N. Saranya and S. K. Priya, "Deep convolutional neural network feed-forward and back propagation (DCNN-FBP) algorithm for predicting heart disease using Internet of Things," *Int. J. Eng. Adv. Technol.*, vol. 11, no. 1, pp. 283–287, 2021.

[28] J. Zhang and S. Qu, "Optimization of backpropagation neural network under the adaptive genetic algorithm," *Complexity*, vol. 2021, Jul. 2021, Art. no. 1718234.

[29] H. Fei and L. Zhang, "Prediction model of end-point phosphorus content in BOF steelmaking process based on PCA and BP neural network," *J. Process Control*, vol. 66, pp. 51–58, Jun. 2018.

[30] T. M. Kearney, A. A. K. Fox, J. A. Lee, J. R. Prescott, M. A. Shah, D. P. Batin, W. Baig, S. Lindsay, S. T. Callahan, E. W. Shell, L. D. Eckberg, G. A. Zaman, S. Williams, M. M. J. Neilson, and J. Nolan, "Predicting death due to progressive heart failure in patients with mild-to-moderate chronic heart failure," *J. Amer. College Cardiol.*, vol. 40, no. 10, pp. 1801–1808, 2002.

[31] H. B. Grotenhuis, C. Zhou, G. Tomlinson, K. V. Isaac, M. Seed, L. Grosse-Wortmann, and S.-J. Yoo, "Cardiothoracic ratio on chest radiograph in pediatric heart disease: How does it correlate with heart volumes at magnetic resonance imaging?" *Pediatric Radiol.*, vol. 45, no. 11, pp. 1616–1623, Oct. 2015.

[32] P. Chen, J. Wu, C. Lin, J. Hsu, and N. Pai, "Enhancement of breast mammography to rapid screen abnormalities using 2D spatial fractional-order feature extraction and multilayer machine vision classifier," *IEEJ Trans. Electr. Electron. Eng.*, vol. 17, no. 1, pp. 132–147, Jan. 2022.

[33] Y.-C. Li, T.-Y. Shen, C.-C. Chen, W.-T. Chang, P.-Y. Lee, and C.-C.-J. Huang, "Automatic detection of atherosclerotic plaque and calcification from intravascular ultrasound images by using deep convolutional neural networks," *IEEE Trans. Ultrason., Ferroelectr., Freq. Control*, vol. 68, no. 5, pp. 1762–1772, May 2021.

[34] J.-Y. Lu, P.-Y. Lee, and C.-C. Huang, "Improving image quality for single-angle plane wave ultrasound imaging with convolutional neural network beamforme," *IEEE Trans. Ultrason., Ferroelectr., Freq. Control*, vol. 69, no. 4, pp. 1326–1336, Feb. 2022.

[35] C. L. Schlett, D. C. Kwait, A. A. Mahabadi, F. Bamberg, C. J. O'Donnell, C. S. Fox, and U. Hoffmann, "Simple area-based measurement for multidetector computed tomography to predict left ventricular size," *Eur. Radiol.*, vol. 20, no. 7, pp. 1590–1596, Jul. 2010.

[36] O. A. Centurión, E. K. Scavenius, M. L. Miño, and R. O. Sequeira, "Evaluating cardiomegaly by radiological cardiothoracic ratio as compared to conventional echocardiography," *J. Cardiol. Current Res.*, vol. 9, no. 2, pp. 1–3, 2017.

[37] P. Hota and S. Simpson, "Going beyond cardiomegaly: Evaluation of cardiac chamber enlargement at non- electrocardiographically gated multidetector CT: Current techniques, limitations, and clinical implications," *Radiol., Cardiothoracic Imag.*, vol. 1, no. 1, pp. 1–10, 2019.
[38] S. B. Malik, D. Kwan, A. B. Shah, and J. Y. Hsu, "The right atrium: Gateway to the heart—Anatomic and pathologic imaging findings," *RadioGraphics*, vol. 35, no. 1, pp. 14–31, Jan. 2015.
[39] M. Abd-Hazaa, S. Sharif, and A. A.-H. Kadhum, "Validity of chest X-ray in estimation of cardiac size in comparison to echocardiography," *Med. J. Basrah Univ.*, vol. 25, no. 2, pp. 48–51, Dec. 2007.
[40] S. J. Quinton, J. A. Ker, P. Rheeder, and A. Deffur, "The reliability of chest radiographs in predicting left atrial enlargement," *CardioVascular J. Afr.*, vol. 21, no. 5, pp. 274–279, Oct. 2010.
[41] S. Singal-Parulkar, S. Jamot, and Z. Hussain, "An atypical case of dysphagia: Left atrial enlargement," *Amer. J. Gastroenterol.*, vol. 113, pp. S1013–S1014, Oct. 2018.

JIAN-XING WU was born in 1985. He received the B.S. and M.S. degrees in electrical engineering from the Southern Taiwan University of Science and Technology, Tainan City, Taiwan, in 2007 and 2009, respectively, and the Ph.D. degree in biomedical engineering from the National Cheng Kung University, Tainan City, in 2014.

He was a Postdoctoral Research Fellow with the X-ray and IR Imaging Group, National Synchrotron Radiation Research Center, Hsinchu City, Taiwan, from 2014 to 2017. He was also a Postdoctoral Research Fellow with the Department of Niche Biomedical LLC, California NanoSystems Institue, UCLA, Los Angeles, USA, from 2017 to 2018. He has been an Assistant Professor with the Department of Electrical Engineering, National Chin-Yi University of Technology, Taichung City, Taiwan, since 2019. His research interests include artificial intelligence applications in electrical engineering and biomedical engineering, biomedical signal processing, medical ultrasound, and medical device design, X-ray microscopy.

CHING-CHOU PAI was born in Tainan City, Taiwan, in 1975. He received the M.D. degree from the National Defense Medical Center, Taipei City, Taiwan, in 2001. He is currently pursuing the M.S. degree with the Department of Electrical Engineering, National Chin-Yi University of Technology, Taichung City.

He completed the Residency and Fellowship training in cardiovascular surgery at Tri-Service General Hospital, Taipei City, in 2010. He was an Attending Physician with the Department of Surgery, Chi-Mei Hospital, from 2012 to 2016. He is currently an Attending Physician with the Department of Surgery Show-Chwan Memorial\Hospital, Changhua, Taiwan. His research interests include open aortic surgery, aortic stent graft implantation, intervention of peripheral arterial and venous disease, and digital image processing.

CHUNG-DANN KAN received the M.D. degree from the Kaohsiung Medical College, Kaohsiung City, Taiwan, in 1993, and the Ph.D. degree from the National Cheng Kung University, Tainan City, Taiwan, in 2010. He completed the Residency and Fellowship training in cardiovascular surgery at National Cheng Kung University Hospital, Tainan City. He is currently an Attending Physician with the Department of Surgery, National Cheng Kung University Hospital, and the Institute of Clinical and Cardiovascular Research Center, Medical College, Tainan City. He has been a Professor with the Department of Surgery, National Cheng Kung University, since 2019. His research interests include cardiac regeneration and aortic stent graft.

PI-YUN CHEN received the Ph.D. degree from the Graduate School of Engineering Science and Technology, National Yunlin University of Science & Technology, Yunlin, Taiwan, in 2011.

Since 2019, she has been the Chief of the Department of Electrical Engineering, National Chin-Yi University of Technology, Taichung City, Taiwan, where she is currently an Associate Professor with the Department of Electrical Engineering. Her current research interests include neural network computing and its applications, fuzzy systems, and advanced control systems.

WEI-LING CHEN was born in Kaohsiung City, Taiwan, in 1970. She received the B.S. degree in mechanical engineering, and the M.S. and Ph.D. degrees in biomedical engineering from the National Cheng Kung University, Tainan, Taiwan, in 1994, 1996, and 2015, respectively.

She was worked with the Department of Engineering and Maintenance, Kaohsiung Veterans General Hospital, Kaohsiung City, Taiwan, from 2013 to 2018, and also with the KSVGH Originals & Enterprises, Kaohsiung Veterans General Hospital, Kaohsiung City, from 2018 to 2020. Since 2020, she has been working the Institute Food and Drug Administration, Ministry of Health Welfare, Taipei County, Taiwan. Since 2021, she has also been an Assistant Professor with the School of Biomedical Engineering, College of Biomedical Engineering, Taipei Medical University, Taipei. Her research interests include biomedical signal processing, hemodynamic analysis, healthcare, numerical analysis, medical device design, and numerical analysis.

CHIA-HUNG LIN was born in Kaohsiung City, Taiwan, in 1974. He received the B.S. degree in electrical engineering from the Tatung Institute of Technology, Taipei City, Taiwan, in 1998, and the M.S. and Ph.D. degrees in electrical engineering from the National Sun Yat-sen University, Kaohsiung City, in 2000 and 2004, respectively.

He was a Professor with the Department of Electrical Engineering, Kao-Yuan University, Kaohsiung City, from 2004 to 2017. He has been a Professor with the Department of Electrical Engineering, since 2018. His research interests include neural network computing and its applications in power system and biomedical engineering, biomedical signal and image processing, healthcare, hemodynamic analysis, and pattern recognition.